Electronic Supplementary Material (ESI) for New Journal of Chemistry.

Supporting information

Nanoscale cobalt metal-organic framework as a catalyst for visiblelight-driven and electrocatalytic water oxidation

Qian Xu,[a] Hui Li,[a] Fan Yue,[a]Le Chi,[a] Jide Wang[*a]

[a] Ministry Key Laboratory of oil and Gas Fine Chemical, College of Chemistry and Chemical Engineering Xinjiang University

Experimental and calculation

Quantum yield calculation

Initial O_2 formation rate=2.22×10^{19} mol s^{-1}

Photon flux=$26.4\times(\frac{\pi\times D\times l}{2})\times6.34\times10^{20}$ mol s^{-1}

$=26.4\times(\frac{3.14\times2\times3.5}{2})\times6.34\times10^{20}$ mol s^{-1}

$=1.84\times10^{20}$ mol s^{-1}

$\Phi_{QY(initial)}=2\times\frac{Initial\ \ O_2\ \ formation\ \ rate}{photon\ \ \ flux}$

$=2\times\frac{2.22\times10^{19}}{1.84\times10^{20}}\times100\%$

$=24.2\%$

Material

Tri(2,2’-bipyridine)ruthenium(II) chloride hexahydrate (98.0%) was purchased from Tci.

Preparation of different kinds of photosensitizers

Synthesis of $[Ru(bpy)_3]SO_4$

$[Ru(bpy)_3]SO_4$ was synthesized according to reference1. 1 equiv of Ag_2SO_4 was added to an aqueous solution of $[Ru(bpy)_3]Cl_2$ and stirred vigorously for 1 hour.Solid and liquid were separated by filtration.After evaporation of the aqueous solution under reduced pressure,orange solid photosensitizer was obtained.

Synthesis of $[Ru(bpy)_3](ClO_4)_2$

$[Ru(bpy)_3](ClO_4)_2$ was synthesized according to reference 2.The 4 M $HClO_4$ was adding to an aqueous solution of $[Ru(bpy)_3]Cl_2$ and then separated by filtration.

Synthesis of $[Ru(bpy)_3](ClO_4)_3$

$[Ru(bpy)_3](ClO_4)_3$ was prepared according to reference3.The salt of $[Ru(bpy)_3](ClO_4)_2$ was dissolved in 0.5 M H_2SO_4.A scoop of PbO_2 was added,and the solution was stirred at room temperature and filtered through a fine frit.The perchlorate concentration of filtrate was adjusted to ~2 M by the dropwise addition of $HClO_4$,and the solution was then cooled in an ice bath.Green crystals of $[Ru(bpy)_3](ClO_4)_3$ rapidly formed and were recrystallized from 4 M $HClO_4$ at0^{o}C.

Synthesis of ZIF-67

800 nm ZIF-67. 3.321 gof $Co(Ac)_2 \cdot 4H_2O$ and 3.284 g of 2-methylimidazole were each dissolved in 100 mL methanol at room temperature. The former salt solution was poured into the latter ligand solution under vigorous stirring.The mixture was stirred for 30 min and then kept for 24 h.The solid product was separated by centrifugation and washed with methanol three times,followed by vacuum during at 70^{o}C for 8 h.

1.7 **μm ZIF-67.** Typically, 1.436 g $Co(NO_3)_2 \cdot 6H_2O$ and 3.244

g of 2-methylimidazole were each dissolved in 100 mL methanol at 60^{o}C. The former salt solution was poured into the latter ligand solution under vigorous stirring.The mixture was stirred for 30 min and then kept for 24 h.The solid product was separated by centrifugation and washed with methanol three times,followed by vacuum during at 70^{o}C for 8 h.

Oxygen Evolution Quantified by GC

Photocatalytic water oxidation was performed as follows.The Co-ZIF-67 was added to a buffer solution (80 mM,pH=7.0-10.0 for borate buffer;80 mM,pH 9.0 for phosphate and carbonate buffer) containing $Na_2S_2O_8$(40mM) and $[Ru(bpy)_3](ClO_4)_2$ (1 mM) purged with Ar gas for 10 min in a flask(~20 mL) sealed with a rubber septum.The reaction was started by irradiating the solution with a Xe lamp (300 W,26.4 mW/cm^2) through a transmitting glass filter($\lambda \geq 420$ nm) at room temperature.After each sampling time,100 μL of Ar was injected into the flask and thesame volume of gas sample in the headspace of the flask was withdrawn by a gas tight syringe and used for gas chromatography(GC) analysis.The O_2in the sampled gas was separated by passing through a molecular sieve 5**Å** columns with an Ar carrier gas and quantifies by a Thermal Conductivity Detector (TCD)(Shimadzu GC-14B).The total

amount of evolved O_2 was calculated from the concentration of O_2 in the headspace gas.

Electrochemical Measurements

The working electrode was prepared on a fluorine-doped tin oxide (FTO) transparent conductive film glass. Co-ZIF-67 (8 mg) and Nafion solution (40 μL) were mixed with 1 mL ethanol under sonication for 30 min to get slurry. Next 8 μL of the slurry was transferred onto the FTO glass, and the electrode was dried in air for 24 h. Electrochemical measurements were performed in a typical three electrode cell, using a platinum wire as counter electrode and Ag/AgCl electrode as reference electrode. The electrochemical experiments were taken on a CHI600D workstation. The sweep rate for CVs was 10 mV/s unless otherwise stated.

Characterization of Particles

X-ray photoelectron spectra (XPS) were measured by Kratos Amicus with X-ray monochromatisation.Scanning electron microscope (SEM) images of particles were observed by a Merlin Compact,with scanning voltage at 100000 V.

The product was characterized by X-ray diffraction (XRD) using a Rigaku D/max-ga X-ray diffractometer at a scan rate of 6^o min^{-1} in 2θ ranging from 10^o to 40^o with Cu Kα radiation (λ =

1.54178 Å).

Spectroscopic Measurements

Dynamic light scattering (DLS) measurements were carried out using Zetasizer Nano S90 instrument (Malvern Instruments Ltd.) for reaction solutions. UV-vis absorption spectra were recorded on UV-2550 (Shimadzu).Liquid chromatography mass spectrometer were performed with an HP1100 (Agilent Technologies Inc.) with ESI source.Inductively coupled plasma optical emission spectrometry was carried out on a PerkinElmer instruments (ICP-4300DV) and measured cobalt concentration in the liquid phase.

DFT calculation

Theoretical calculations were carried out using DFT as implemented in Gaussian 03. Full geometry optimization computations were performed using the Tao-Perdew-Staroverov-Scuseria (TPSS) method and the 6-31G (d, p) basis set was used for C, H, N, O atoms and the LanL2DZ set with an effective core potential for Co atom. Harmonic vibrational frequency analysis confirmed that the initial state and final state had no imaginary frequency and transition state structure had only one imaginary frequency. Intrinsic reaction coordinate (IRC) calculations also confirmed that the latter

connected reactants and products. The gas-phase free energies, G, were obtained at T=298.15 K at optimized structures.

Table.S1 Photocatalytic water oxidation catalyzed by cobalt species

Catalyst	Oxidation	pH	TOF	Ref.
Co-ZIF-67	Light[a]	9.0	0.035	This work
Co_3O_4	Light[a]	9.0	0.0099	This work
SBA-15/Co_3O_4	Light[a]	5.8	0.01[c]	4
$NiCo_2O_4$	Light[a]	5.0	0.00007	5
Co_3O_4/SiO_2-60	Light[a]	9.0	0.0009 [b]	6

a) Using $[Ru(bpy)_3]^{2+}/S_2O_8^{2+}$. b) In mol O_2 s^{-1}("surface Co site")$^{-1}$~16% of thecobalt was estimated to be on the surface.c) per cobalt atom

Table S2. TON, TOF and quantum yield of photocatalytic water oxidation catalyzed by different catalysts[a].

Catalyst	Representative reaction conditions	TON	TOF	$\Phi_{QY(initial)}$ %	Ref.
Co-ZIF-67	Xe lamp (λ≧420 nm); 0.5 mg catalyst; 1.0 mM $[Ru(bpy)_3](ClO_4)_2$; 40 mM $Na_2S_2O_8$; 80 mM sodium borate buffer (pH=9.0)	52.5	0.035 s^{-1}	24.2	This work
$Co_3[Fe(CN)_6]_2 \cdot 14\ H2O$	LED lamp, 470 nm; 10 mg catalyst; 1.0 mM $[Ru(bpy)_3]^{2+}$; 5 mM $Na_2S_2O_8$; 100 mL of pH=7.0 phosphate buffer	No data	3.0×10^{-4} s^{-1}	88	7
SBA-15/Co_3O_4	Ar ion laser, 476 nm; 200 mg	No data	0.01 s^{-1}	18	8

	catalyst; 45 mg $[Ru(bpy)_3]Cl_2$ 6 H_2O; 130 mg $Na_2S_2O_8$; 40 mL aqueous buffer (Na_2SiF_6-$NaHCO_3$, 0.022-0.028 M)				
Co_3O_4(nano cages)	LED lamp, λ>420 nm; 0.50 g Ł$^{-1}$ catalyst; 5.0 mM $Na_2S_2O_8$; 1.0 mM $[Ru(bpy)_3]Cl_2$;phosphate buffer solution (pH 7.0, 15 mL)	No data	3.2×10^{-4} mol_{O2} mol_{metal}^{-1} s^{-1}	No data	9
α-Fe_2O_3	200 W Xe lamp, λ>420 nm; 2 mg catalyst; 0.4 mM $[Ru(bpy)_3]Cl_2$; 4 mM $Na_2S_2O_8$; 30 mM sodium borate (pH=8)	0.22 (Nanoparticles)	2.5 ×10^{-4} s^{-1}	No data	10

MIL-101 (Fe)	Xe lamp (λ≧420 nm); 1.0 mg catalyst; 1.0 mM $[Ru(bpy)_3](ClO_4)_2$; 20 mM $Na_2S_2O_8$; 80 mM sodium borate buffer (pH=9.0)	No data	0.01 s^{-1}	20.56	11
$[Co^{II}(Me_6tren)(OH_2)]^{2+}$	Xe lamp (λ>420 nm); 50μM catalyst; 0.5 mM $[Ru(bpy)_3](ClO_4)_2$; 10 mM $Na_2S_2O_8$; pH=8.0 phosphate buffer	54	No data	32	12
$Cs_9[(\gamma\text{-}PW_{10}O_{36})_2Ru_4O_5$（OH)$(H_2O)_4]$	Xe lamp (420-520 nm); 5.1μM catalyst; 1.0 mM $[Ru(bpy)_3]Cl_2$; 10 mM $Na_2S_2O_8$; 20 mM Na_2SiF_6 buffer (pH=5.8)	120	0.13 s^{-1}	No data	13

$[CoMo_6O_{24}H_6]^{3-}$	300 W Xe (400-800 nm); 3.6 mM Catalyst; 0.06 mM $[Ru(bpy)_3](NO_3)_2 \cdot 3H_2O$; 3 mM $Na_2S_2O_8$; 0.1 M borate buffer (pH=8, 10 mL)	107	No date	13	14
$Co_3(O_3PCH_2\text{-}NC_4H_7\text{-}CO_2)_2 \cdot 4H_2O$	300 W Xe (λ≧420 nm); 0.14 g L^{-1}; 1.0 mM $[Ru(bpy)_3]^{2+}$; 5.0 mM $Na_2S_2O_8$; 40 mM borate buffer (pH=9.0)	No date	7.1 μmol s^{-1} g^{-1}	25 (at the 460 nm)	15
$Na_{24}[Ni_{12}(OH)_9(CO_3)_3(PO_4)(SiW_9O_{34})_3] \cdot 56H_2O$	300 W Xe lamp (λ>420 nm); 2 μM catalyst; 1.0 mM $[Ru(bpy)_3]^{2+}$; 5.0 mM $Na_2S_2O_8$; 80 mM borate buffer (pH=9.0)	85.6	0.13 s^{-1}	No data	16

$[Co_4(H_2O)_2(PW_9O_{34})_2]^{10-}$	Xe lamp, 420-470, 16.8 mW light beam with a diameter of ~0.75 cm focused on the reaction solution; 5 μM catalyst; 1.0 mM $[Ru(bpy)_3]^{2+}$; 5.0 mM $Na_2S_2O_8$; 80 mM sodium borate buffer (initial pH 8.0); total reaction volume 2 mL	224 ±11	No data	0.30 ± 0.05	17
$[\{Co_4(OH)_3(PO_4)\}_4(GeW_9O_{34})_4]^{32-}$	300 W Xe lamp, 420-800 nm; 20 μM catalyst; 1.0 mM $[Ru(bpy)_3]^{2+}$; 5.0 mM $Na_2S_2O_8$; sodium borate buffer pH 9.0 (80 mM); total reaction	38.75	0.105 s^{-1}	No data	18

	volume 20 mL				
$[\{Ru_4O_4(OH)_2(H_2O)_4\}(\gamma\text{-}SiW_{10}O_{36})_2]^{10-}$	Xe lamp, 420-520 nm, 50 mW light beam with a diameter of ~1.5 cm focused on the reaction solution; 5.0 μM catalyst ; 1.0 mM $[Ru(bpy)_3]^{2+}$; 5.0 mM $Na_2S_2O_8$; 20 mM sodium phosphate buffer (initial pH 7.2); total reaction volume 8 mL	180	0.08 s^{-1}	38	19
$[Co_4(H_2O)_2(PW_9O_{34})_2]^{10-}$	455 nm LED light (17 mW, beam diameter ~0.5 cm); 2 μM catalyst ; 1.0 $[Ru(bpy)_3]^{2+}$; 5.0 mM $Na_2S_2O_8$; 80	302 ±1	No data	No data	20

	mM sodium borate buffer pH=8.0				
[Ru(bda)(pic)$_2$]	300 W Xe lamp coupled to a 400 nm long-pass filter; 10^{-4} M catalyst; 1.5×10^{-3} M [CD-Ru(bpy)$_3$]$^{2+}$; sodium persulfate 6.67×10^{-2} M in 5 mL phosphate buffer solution (pH 7.1, 50 mM) containing 10% acetonitrile under visible light irradiation	267	0.13 s^{-1}	84 (at 450 nm)	21
$K_7[Co^{III}Co^{II}(H_2O)W_{11}O_{39}]$	LED lamp, $\lambda>420$ nm; 15 μM catalyst; 5.0 mM $Na_2S_2O_8$; 1.0 mM $[Ru(bpy)_3]Cl_2$; 80	51	0.5 s^{-1}	27	22

			mM sodium borate buffer (initial pH 9.0); total reaction solution volume 18 mL

[a] TOF=TON/60 s, TON=The total number of moles of oxygen per mole of precatalyst. $\Phi_{QY(initial)}$=[(initial O_2 formation rate)/(photon flux)]

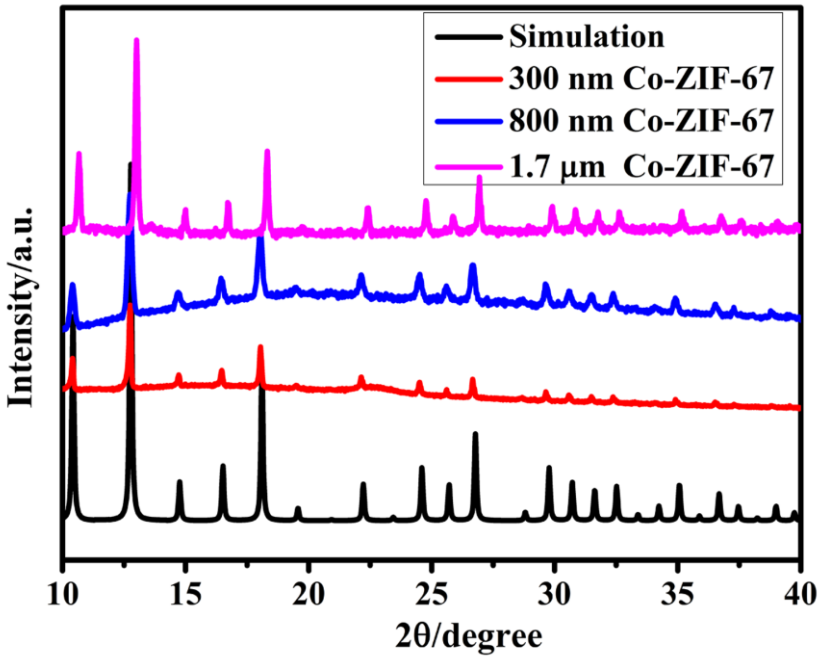

Figure S1. XRD patterns of Co-ZIF-67

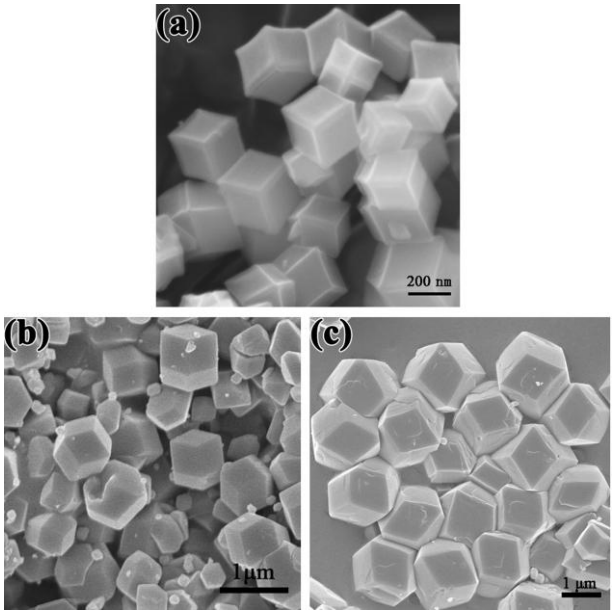

Figure S2. SEM images of the Co-ZIF-67 catalyst with various sizes (a) 300 nm (b) 800 nm (c) 1.7 µm.

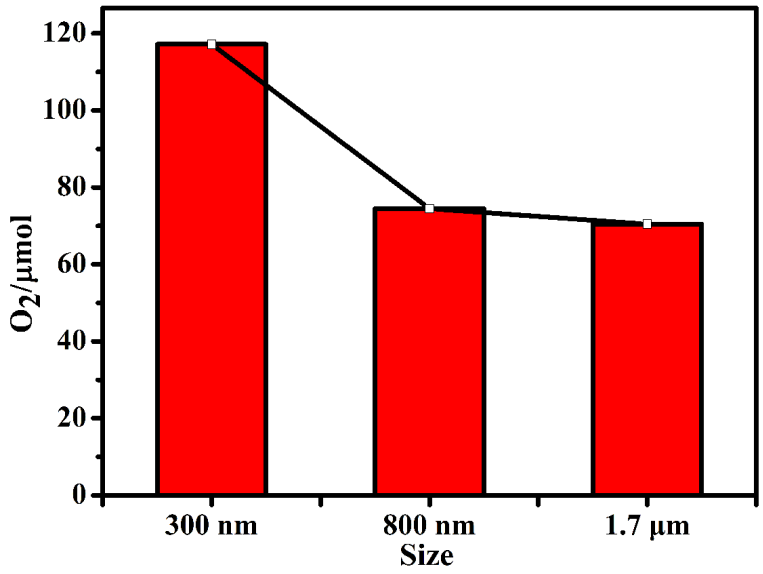

Figure S3. Promotion of photocatalytic oxygen evolution over Co-ZIF-67 under different sizes (300 nm, 800 nm, and 1.7 μm). Conditions: Xe lamp(λ≥420 nm,26.4 mW/cm^2); catalyst, 0.5 mg; 1.0 mM$[Ru(bpy)_3](ClO_4)_2$; 40.0 mM $Na_2S_2O_8$;80 mM sodium borate buffer(initial pH 9.0); total reaction volume 10 mL;vigorous stirring.

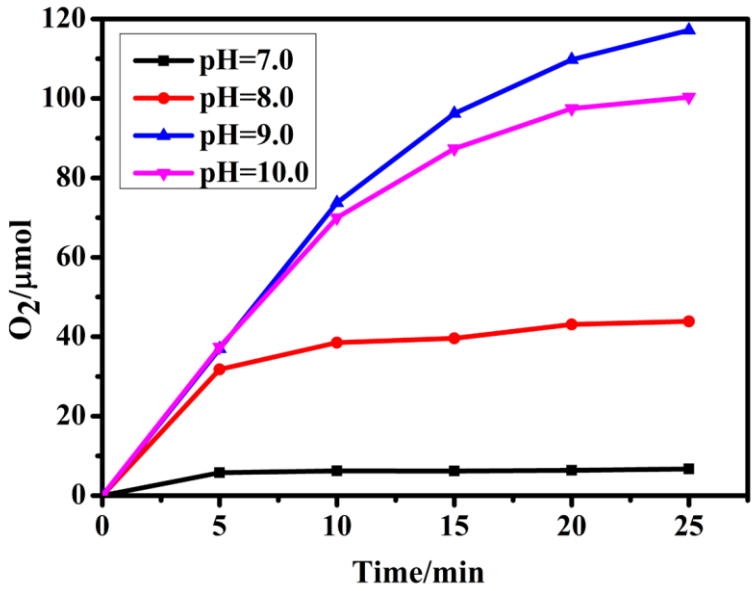

Figure S4. Kinetics of O_2 evolution in the photocatalytic system at various pH values (pH=9.0,blue;pH=10.0,pink;pH=8.0,red;pH=7.0,black). Conditions:Xe lamp(λ≥420 nm,26.4 mW/cm^2); catalyst, 0.5 mg; 1.0 mM $[Ru(bpy)_3](ClO_4)_2$; 40.0 mM $Na_2S_2O_8$;80 mM sodium borate buffertotal reaction volume 10 mL;vigorous stirring.

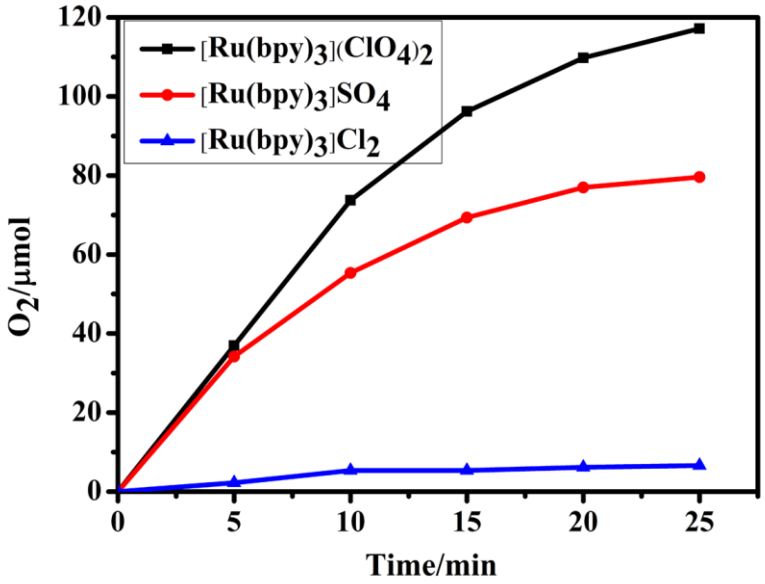

Figure S5. Kinetics of O_2 evolution in the photocatalytic system using different photosensitizers (1.0 mM $[Ru(bpy)_3](ClO_4)_2$,black; 1.0 mM $[Ru(bpy)_3]SO_4$,red; 1.0 mM $[Ru(bpy)_3]Cl_2$,blue).

Conditions:Xe lamp($\lambda \geq 420$ nm,26.4 mW/cm^2); catalyst, 0.5 mg; 40.0 mM $Na_2S_2O_8$; 80 mM sodium borate buffer (initial pH 9.0);total reaction volume 10 mL;vigorous stirring.

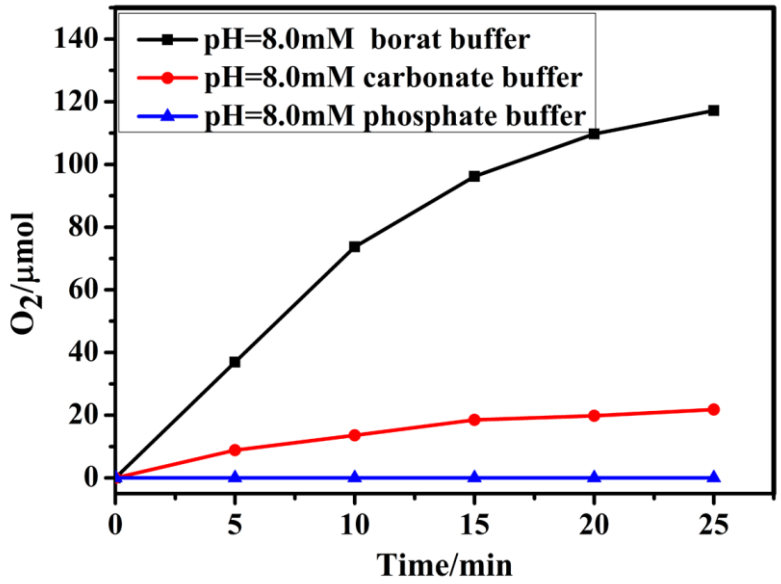

Figure S6. Kinetics of O_2 evolution in the photocatalytic system using different kinds of buffers(pH=9.0,80 mM borate buffer,black;pH=9.0,80 mM phosphate buffer, blue;pH=9.0,80 mM carbonate buffer,red).

Conditions:Xe lamp($\lambda \geq 420$ nm,26.4 mW/cm^2); catalyst, 0.5 mg; 1.0 mM $[Ru(bpy)_3](ClO_4)_2$; 40.0 mM $Na_2S_2O_8$; 80 mM buffer (initial pH 9.0);total reaction volume 10 mL;vigorous stirring.

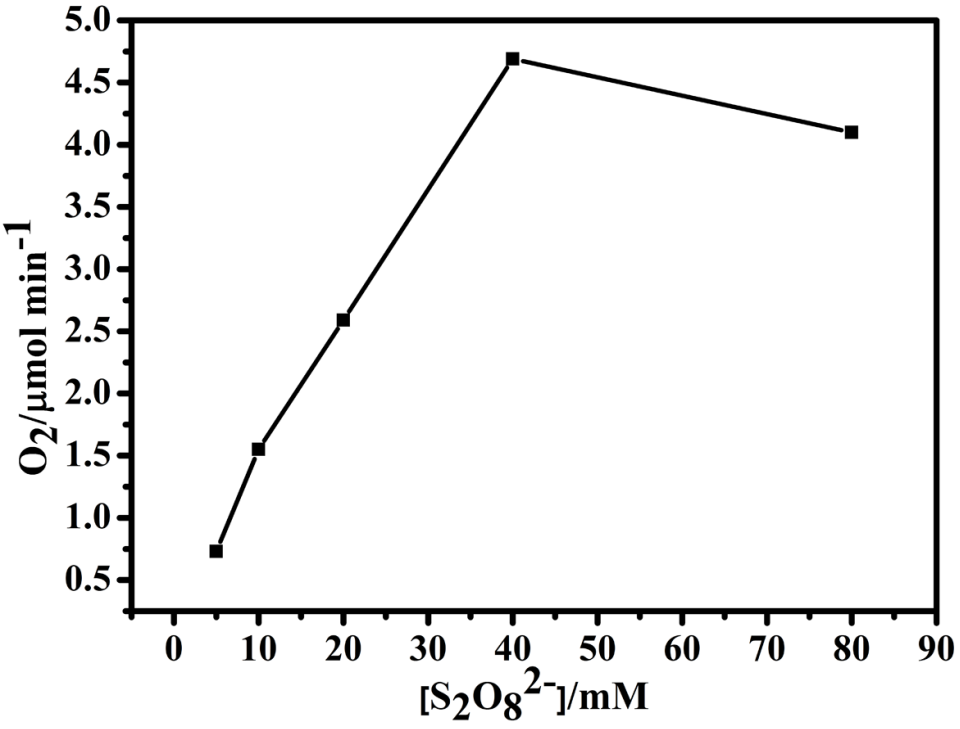

Figure S7. The max O_2 evolution rate [$S_2O_8^{2-}$] for Co-ZIF-67. Conditions: Xe lamp($\lambda \geq 420$ nm,26.4 mW/cm^2); catalyst, 0.5 mg; 1.0 mM[$Ru(bpy)_3$](ClO_4)$_2$; 80 mM sodium borate buffer(initial pH 9.0); total reaction volume 10 mL;vigorous stirring.

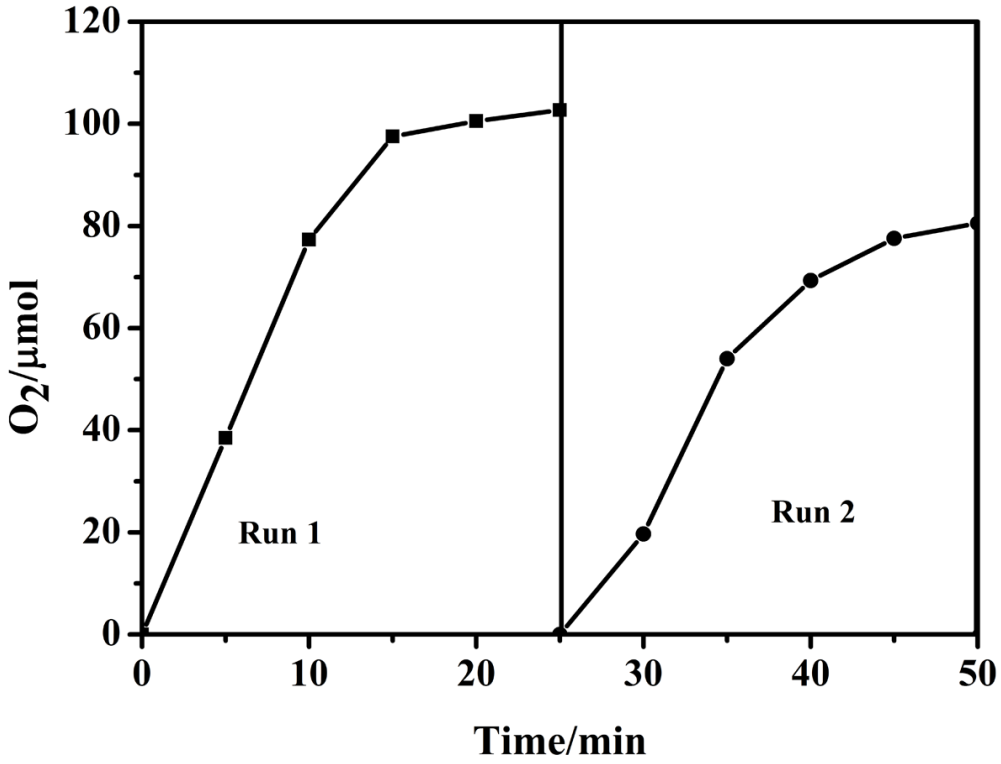

Figure S8. Cycles of the catalytic oxygen evolution in the presence of the Co-ZIF-67 catalyst.

Conditions: Xe lamp($\lambda \geq 420$ nm,26.4 mW/cm^2); catalyst, 0.5 mg; 1.0 mM$[Ru(bpy)_3](ClO_4)_2$; 40 mM $Na_2S_2O_8$; 80 mM sodium borate buffer(initial pH 9.0); total reaction volume 10 mL;vigorous stirring.

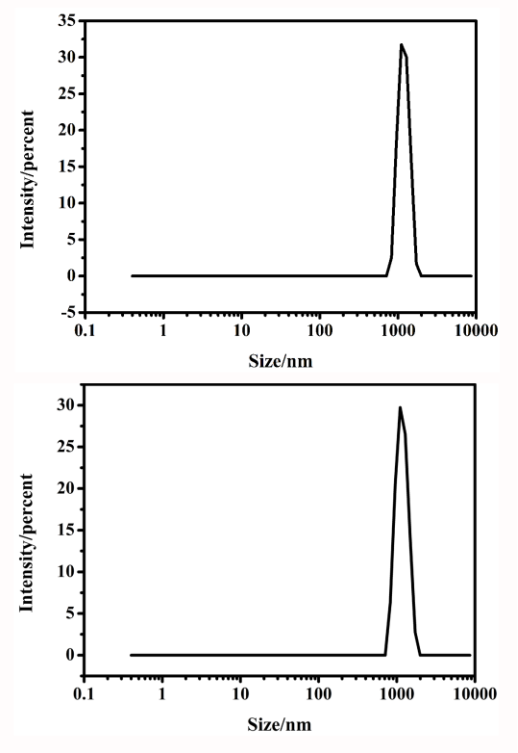

Figure S9. Dynamic light scattering (DLS) characterization of a water oxidation reaction solution before irradiation (top, reference experiment) and of the solution after catalysis (bottom).

Control experiments to exclude RuO_2 as a catalytically active species were performed by replacing Co-ZIF-67 with Ru-containing test compounds (RuO_2 (MW: 133.7 g/mol) and $RuCl_3$ $6H_2O$ (MW: 207.43 g/mol)).

10% of PS decomposition was modeled using 0.1 mM RuO_2. Parallel test were performed replacing RuO_2 with $RuCl_3$ $6H_2O$ under equivalent conditions.

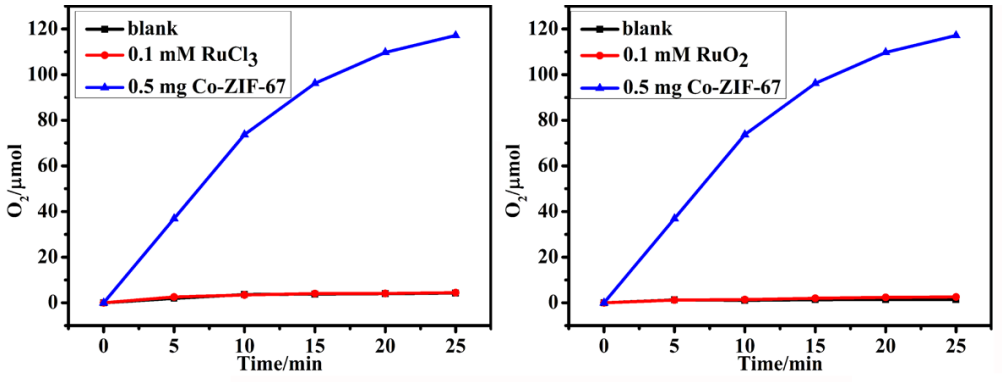

Figure S10. Kinetics of visible-light-driven O_2 evolution for representative WOC tests with 0.5 mg Co-ZIF-67 catalyst compared to: replacement of Co-ZIF-67 with 0.1 mM RuO_2 (right) and replacement of Co-ZIF-67 with 0.1 mM of $RuCl_3$ $6H_2O$ (left; conditions: Xe lamp($\lambda \geq 420$ nm,26.4 mW/cm^2);1.0 mM$[Ru(bpy)_3](ClO_4)_2$; 40 mM $Na_2S_2O_8$; 80 mM sodium borate buffer(initial pH 9.0); total reaction volume 10 mL;vigorous stirring.)

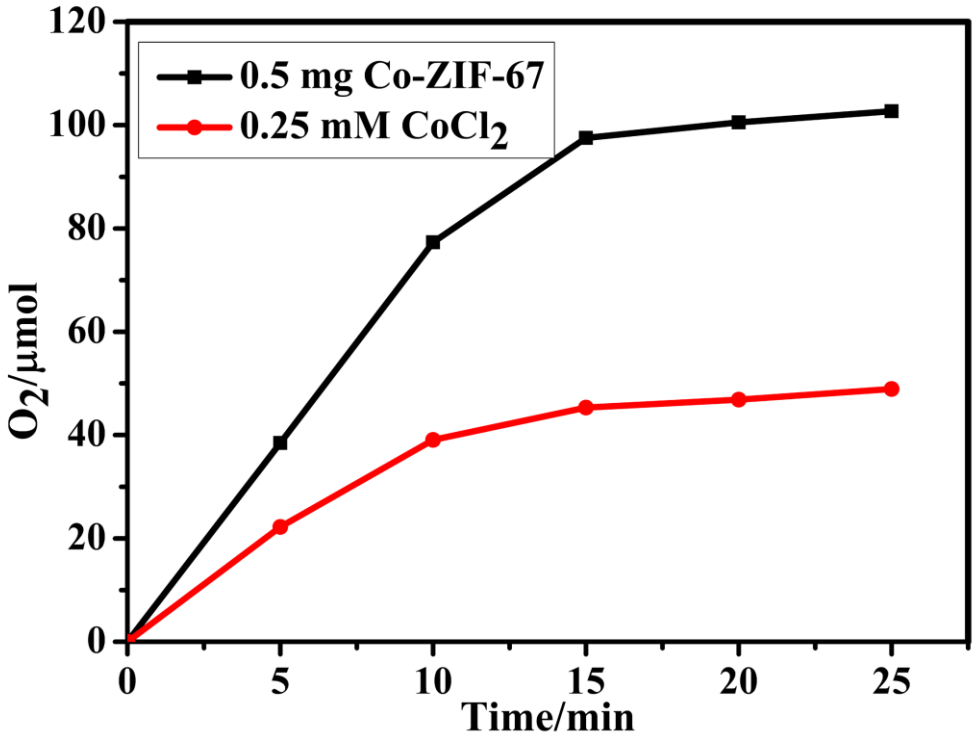

Figure S11. Kinetics of O_2 evolution in the photocatalytic system using Co-ZIF-67 (0.5 mg) and $CoCl_2$ $6H_2O$ (0.25 mM). Conditions: Xe lamp($\lambda \geq 420$ nm,26.4 mW/cm^2);1.0 mM$[Ru(bpy)_3](ClO_4)_2$; 40 mM $Na_2S_2O_8$; 80 mM sodium borate buffer(initial pH 9.0); total reaction volume 10 mL;vigorous stirring.

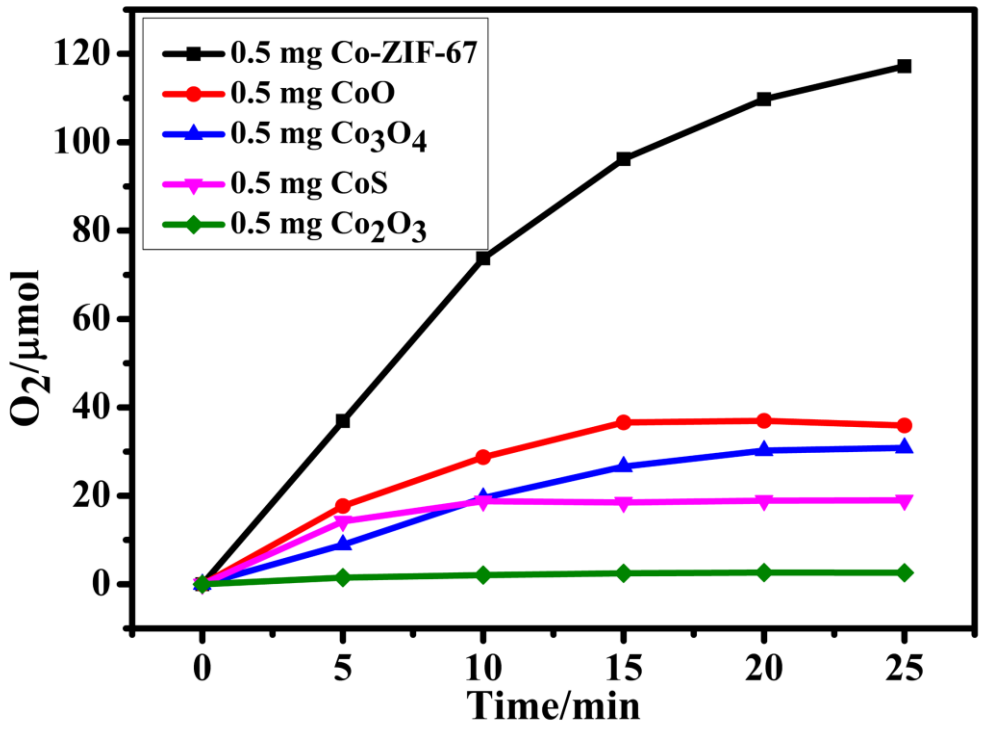

Figure S12. Kinetics of O_2 evolution in the photocatalytic system using Co-ZIF-67 (black), CoO (red), Co_3O_4 (blue), CoS (pink), Co_2O_3 (green).

Conditions: Xe lamp($\lambda \geq 420$ nm,26.4 mW/cm^2);1.0 mM$[Ru(bpy)_3](ClO_4)_2$; 40 mM $Na_2S_2O_8$; 80 mM sodium borate buffer(initial pH 9.0); total reaction volume 10 mL;vigorous stirring.

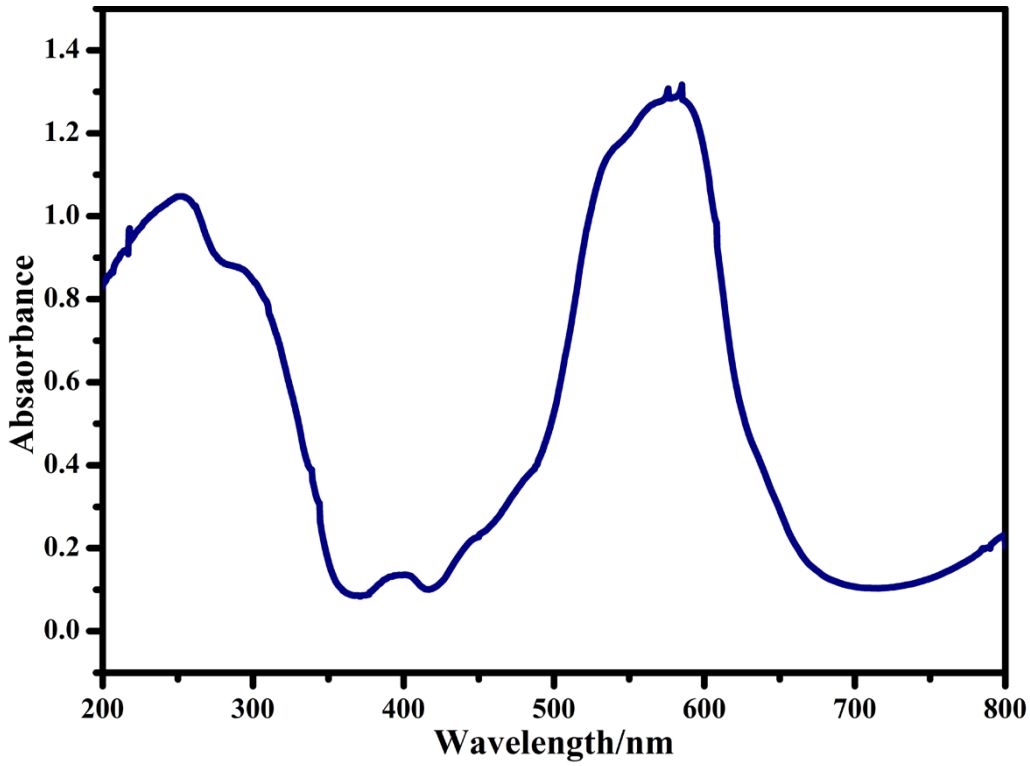

Figure S13. UV-vis absorption spectra of Co-ZIF-67.

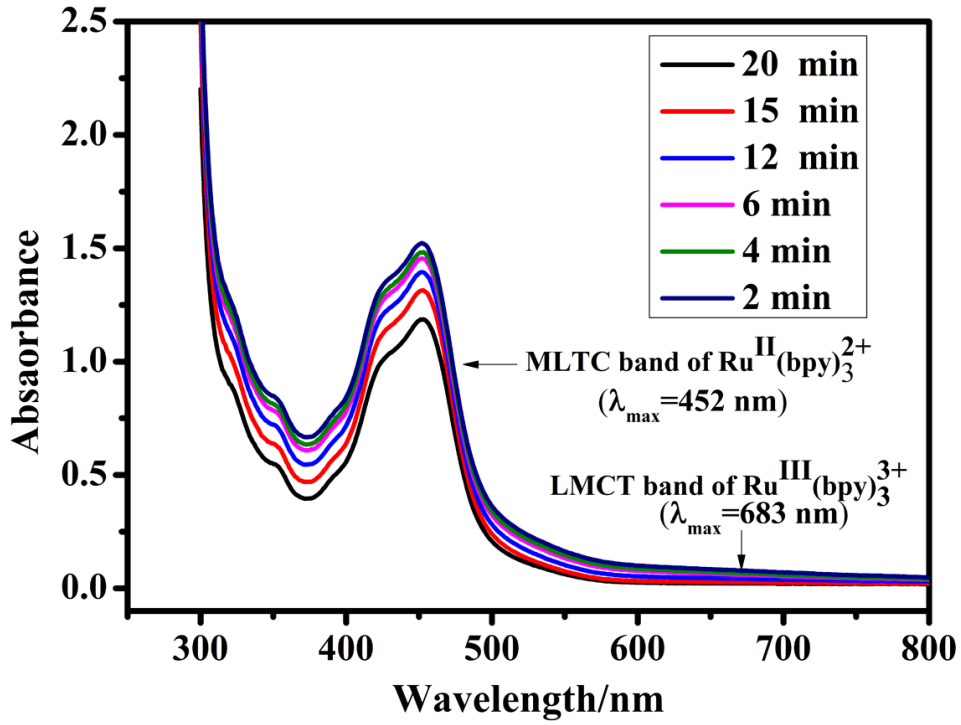

Figure S14. Time-dependent UV-vis absorption spectra after mixing a 0.5 mg Co-ZIF-67 in borate buffer solution and a 0.1mM $[Ru(bpy)_3]^{2+}$ aqueous solution.

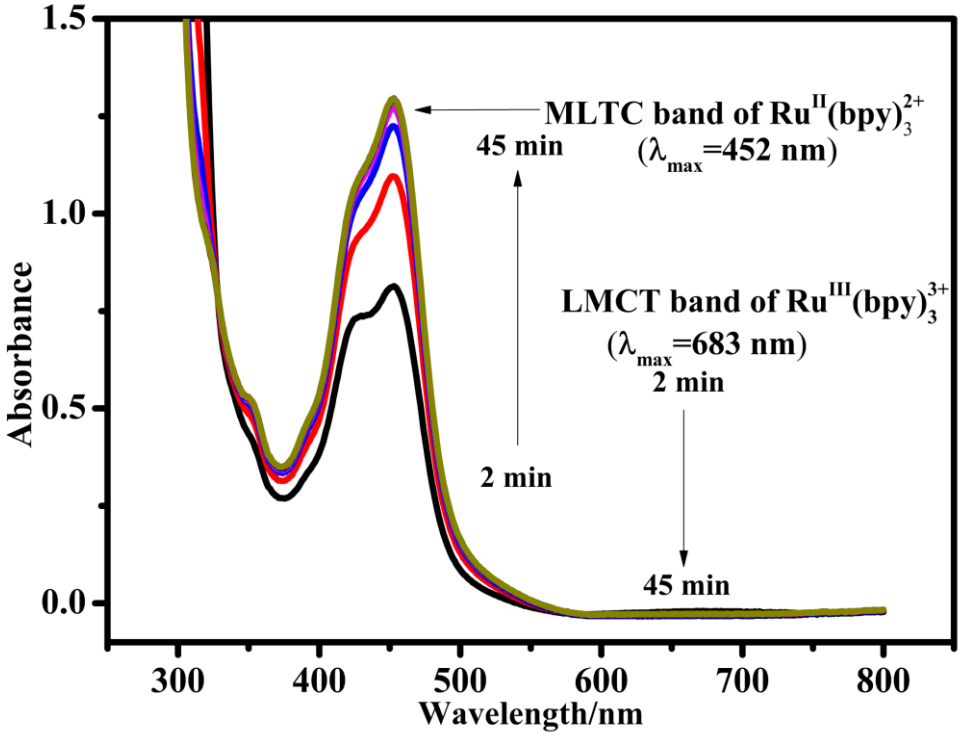

Figure S15. Time-dependent UV-vis absorption spectra of 0.1 mM $[Ru(bpy)_3]^{3+}$ aqueous solution.

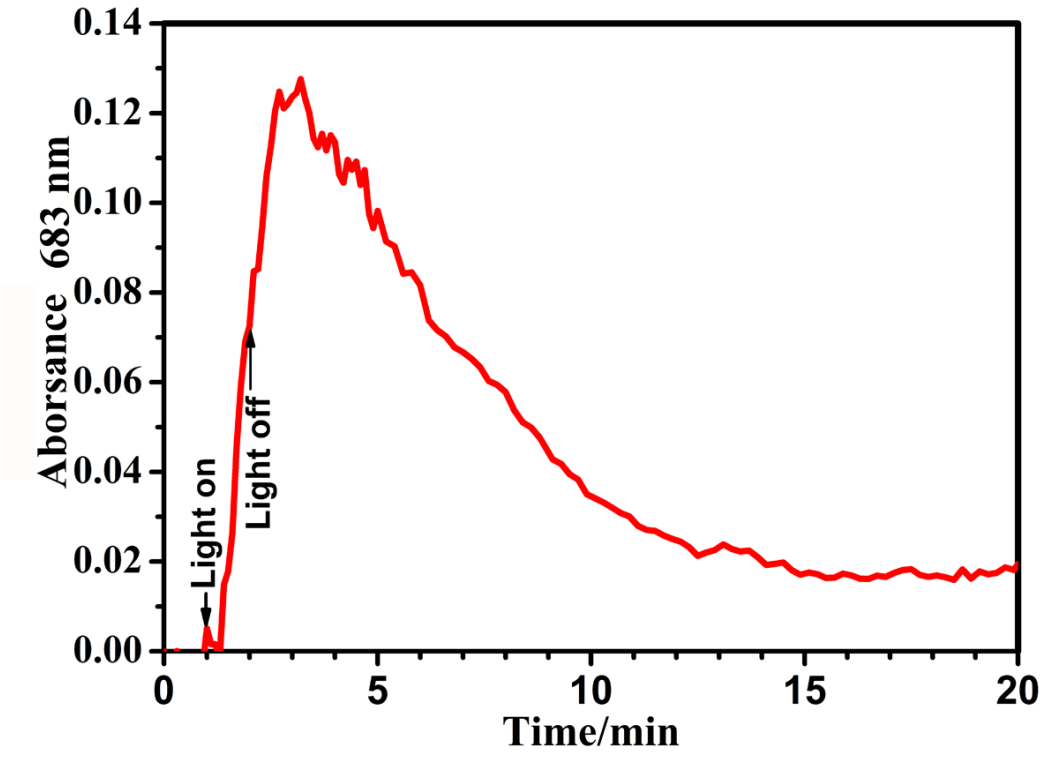

Figure S16. Following photochemical $[Ru(bpy)_3]^{3+}$ formation with the Co-ZIF-67 system.

Conditions: Co-ZIF-67(0.5 mg), $[Ru(bpy)_3](ClO_4)_2$(1.0 mM), $Na_2S_2O_8$(40.0 mM) in 80 mM borate buffer(initial pH 9.0) was kept in the dark in a UV-vis cell.Visible light illumination (Xe lamp, $\lambda \geq 420$ nm,26.4 mW/cm^2) was applied at the down arrows and stopped at the up arrows.

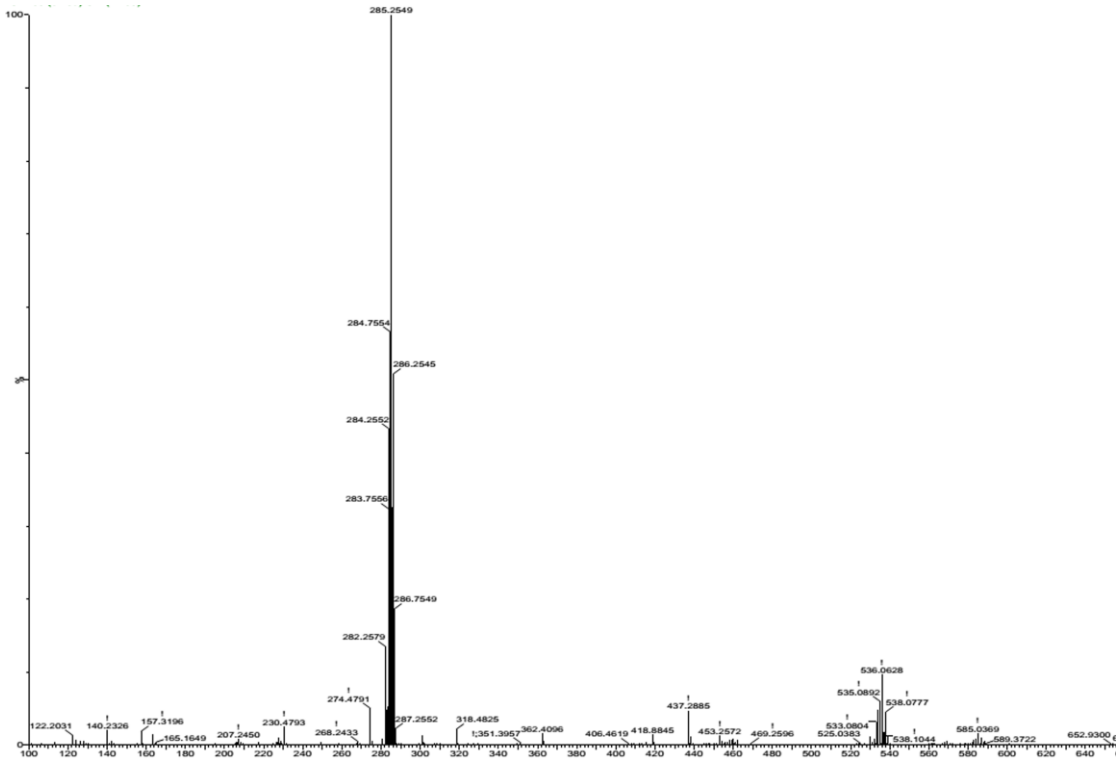

Figure S17. LC-MS of the supernatant post-catalytic solution was recovered by centrifugation.

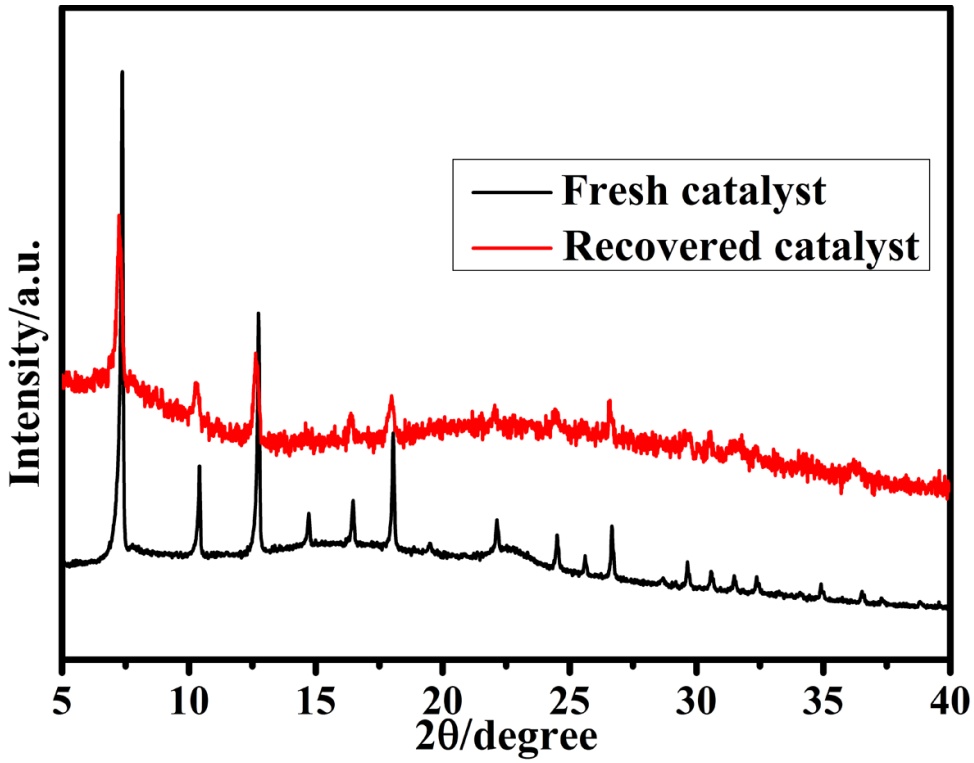

Figure S18. XRD of fresh Co-ZIF-67 (black) and recovered Co-ZIF-67 (red) for photocatalytic.

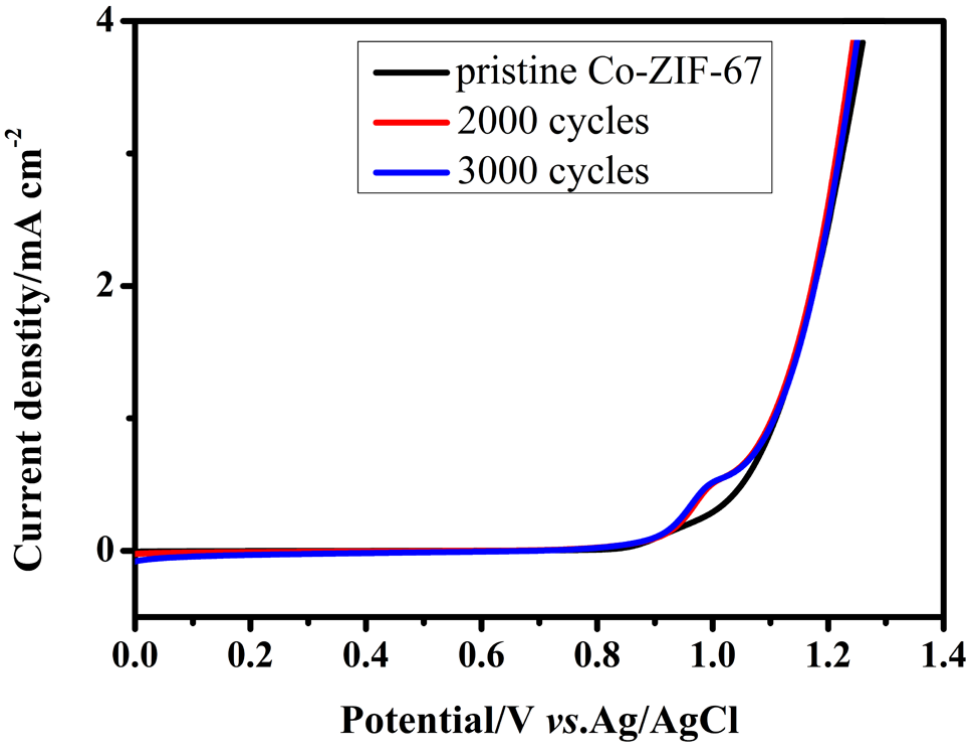

Figure S19.LSV curves of Co-ZIF-67 were recorded before cyclic voltammetry measurements, after 2000 and 3000 cycles.

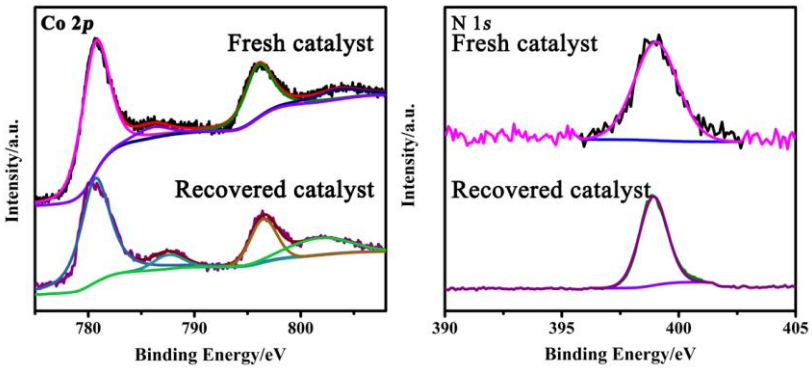

Figure S20. Co 2*p* and N 1*s* XPS spectrums of the catalyst Co-ZIF-67 after CV scans.

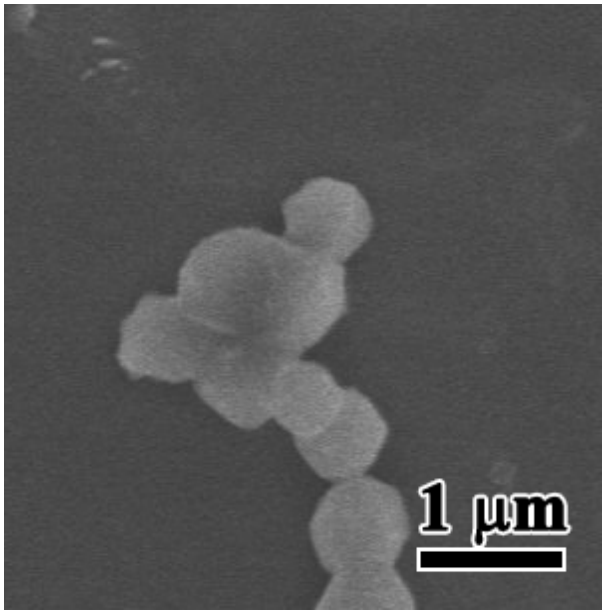

Figure S21. SEM image of the Co-ZIF-67 WOC after photocatalysis in sodium borate buffer (pH=9.0).

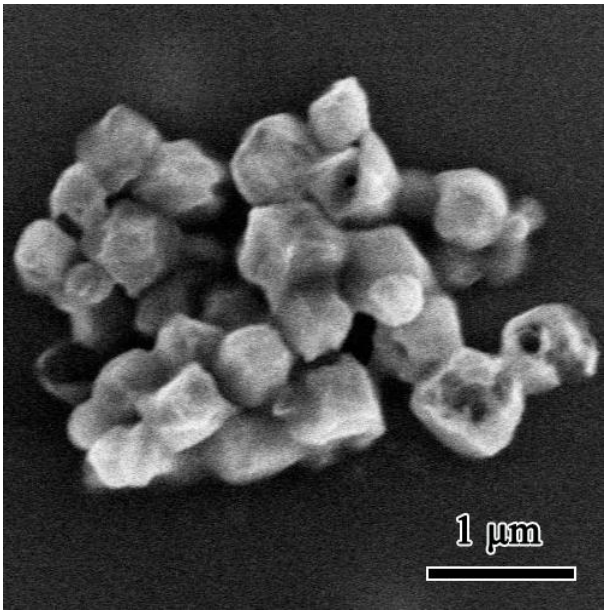

Figure S22. SEM image of the catalyst Co-ZIF-67 after CV scans.

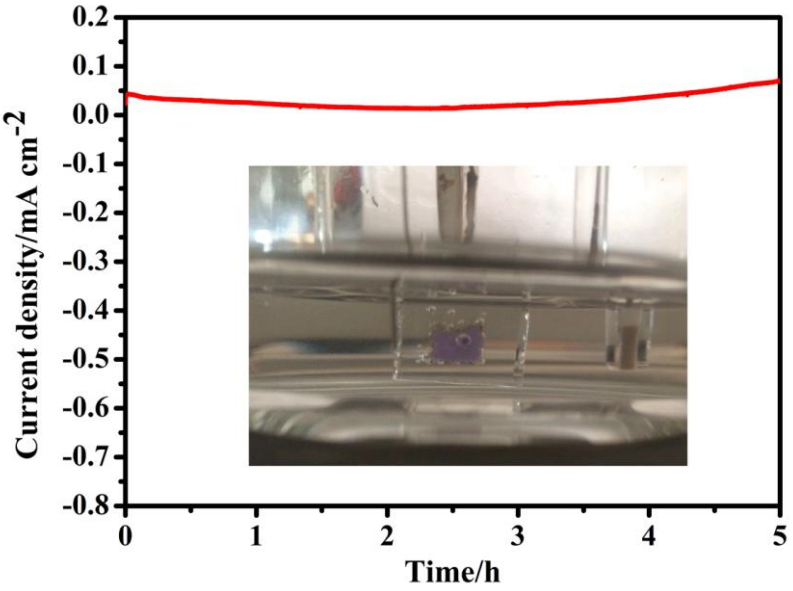

Figure S23. Dependence of current density on time over the Co-ZIF-67/FTO electrode in sodium borate buffer (pH=5.5).

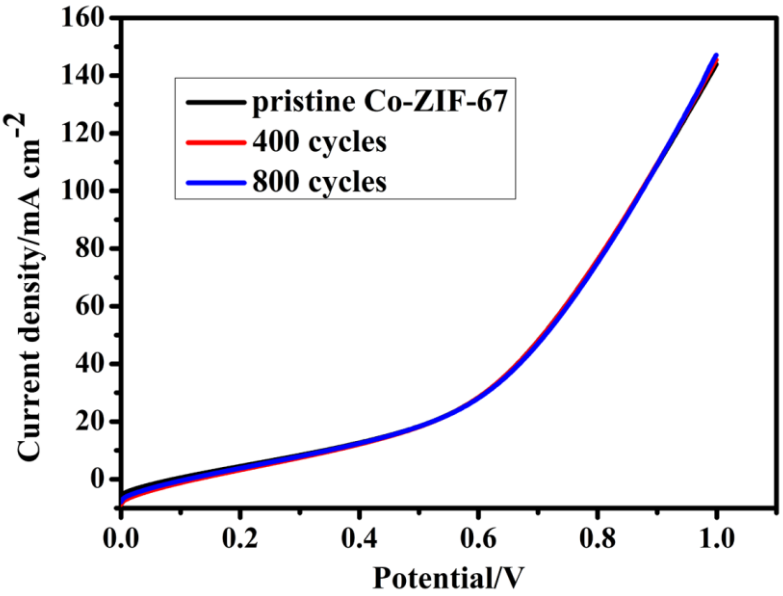

Figure S24. LSV curves of Co-ZIF-67 were recorded before cyclic voltammetry measurements, after 400 and 800 cycles (scan rates: LSV 100 mV s^{-1}).

Note and Reference

1. D. Hong, S. Mandal, Y. Yamada, Y. M. Lee, W. Nam, A. Llobet and S. Fukuzumi, *Inorganic chemistry*, 2013, **52**, 9522-9531.
2. D. Hong, J. Jung, J. Park, Y. Yamada, T. Suenobu, Y.-M. Lee, W. Nam and S. Fukuzumi, *Energy & Environmental Science*, 2012, **5**, 7606.
3. P. K. Ghosh, *journal of american chemical society*, 1984, **106**, 4772-4783.
4. F. Jiao and H. Frei, *Angewandte Chemie*, 2009, **48**, 1841-1844.
5. A. Harriman, I. J. Pickering and J. M. Thomas, *J.Chem.Soc.Faraday Trans*, 1988, **84**, 2795-2806.
6. R. Wu, D. P. Wang, J. Han, H. Liu, K. Zhou, Y. Huang, R. Xu, J. Wei, X. Chen and Z. Chen, *Nanoscale*, 2015, **7**, 965-974.
7. S. Goberna-Ferrón, W. Y. Hernández, B. Rodríguez-García and J. R. Galán-Mascarós, *ACS Catalysis*, 2014, **4**, 1637-1641.
8. F. Jiao and H. Frei, *Angewandte Chemie*, 2009, **48**, 1841-1844.
9. J. Wei, Y. Feng, Y. Liu and Y. Ding, *J. Mater. Chem. A*, 2015, DOI: 10.1039/c5ta06411b.
10. Q. Xiang, G. Chen and T.-C. Lau, *RSC Adv.*, 2015, **5**, 52210-52216.
11. L. Chi, Q. Xu, X. Liang, J. Wang and X. Su, *Small*, 2016.
12. D. Hong, J. Jung, J. Park, Y. Yamada, T. Suenobu, Y.-M. Lee, W. Nam and S. Fukuzumi, *Energy & Environmental Science*, 2012, **5**, 7606-7616.
13. C. Besson, Z. Huang, Y. V. Geletii, S. Lense, K. I. Hardcastle, D. G. Musaev, T. Lian, A. Proust and C. L. Hill, *Chemical communications*, 2010, **46**, 2784-2786.

14. S. Tanaka, M. Annaka and K. Sakai, *Chemical communications*, 2012, **48**, 1653-1655.
15. T. Zhou, D. Wang, S. C.-K. Goh, J. Hong, J. Han, J. Mao and R. Xu, *Energy & Environmental Science*, 2015.
16. X. B. Han, Y. G. Li, Z. M. Zhang, H. Q. Tan, Y. Lu and E. B. Wang, *Journal of the American Chemical Society*, 2015, **137**, 5486-5493.
17. Z. Huang, Z. Luo, Y. V. Geletii, J. W. Vickers, Q. Yin, D. Wu, Y. Hou, Y. Ding, J. Song, D. G. Musaev, C. L. Hill and T. Lian, *Journal of the American Chemical Society*, 2011, **133**, 2068-2071.
18. X. B. Han, Z. M. Zhang, T. Zhang, Y. G. Li, W. Lin, W. You, Z. M. Su and E. B. Wang, *Journal of the American Chemical Society*, 2014, **136**, 5359-5366.
19. Y. V. Geletii, Z. Huang, Y. Hou, D. G. Musaev, T. Lian and C. L. Hill, *Journal of the American Chemical Society*, 2009, **131**, 7522-7523.
20. J. W. Vickers, H. Lv, J. M. Sumliner, G. Zhu, Z. Luo, D. G. Musaev, Y. V. Geletii and C. L. Hill, *Journal of the American Chemical Society*, 2013, **135**, 14110-14118.
21. H. Li, F. Li, B. Zhang, X. Zhou, F. Yu and L. Sun, *Journal of the American Chemical Society*, 2015, **137**, 4332-4335.
22. F. Song, Y. Ding, B. Ma, C. Wang, Q. Wang, X. Du, S. Fu and J. Song, *Energy & Environmental Science*, 2013, **6**, 1170.